Hydrology and Earth System Sciences Discussions

Hydrological effects of the temporal variability of the multiscaling of snowfall on the Canadian prairies

K. R. Shook and J. W. Pomeroy

Centre for Hydrology, University of Saskatchewan, Saskatoon, Saskatchewan, Canada

HESSD

7, 1279–1303, 2010

Temporal variability of snowfall multiscaling

K. R. Shook and
J. W. Pomeroy

Title Page

Abstract	Introduction
Conclusions	References
Tables	Figures

|◄ | ►|
◄ | ►

Back | Close

Full Screen / Esc

Printer-friendly Version

Interactive Discussion

Abstract

Daily historical snowfall data were analysed with the objective of determining the stability of their variability at short temporal scales. The data are weakly multifractal over periods shorter than one month, which controls their scaling properties and which can be used to statistically downscale monthly data to shorter-duration values. Although the daily snowfall values appear to be stationary, their multifractality, as indexed by the universal multifractal parameters shows much temporal variability, with most sites showing statistically-significant trends. Through use of a physically-based model of cold regions hydrology, it is demonstrated that the variability of the multiscaling parameters of snowfall can affect the timing and quantity of snow accumulation and melt in catchments where the snowpacks are subject to wind redistribution, and so trends in scaling based on multifractal characteristics should be taken into account when downscaling climate model scenario outputs.

1 Introduction

The Canadian prairies are a cold, semi-arid region prone to prolonged droughts. Consequently, the potential effects of climate change on water resources are of great interest. Prairie streamflow is dominated by snowmelt runoff and the source snowfalls are subject to wind redistribution by blowing snow which transforms them into highly variable, redistributed snowcovers (Shook and Gray, 1997) and subjects them to substantial sublimation loss (Pomeroy et al., 1993; Pomeroy and Gray, 1995; Fang and Pomeroy, 2008). Predicting future streamflows therefore requires prediction of future snow accumulation and redistribution. Although physically-based hydrological models that incorporate blowing snow processes are required to understand the effects of climate change on prairie hydrology, these models generally need input data such as precipitation, wind speed, air temperature and humidity at hourly temporal resolutions which are coarser than can be simulated by climate models (Wilby and Wigley, 1997)

and some form of temporal downscaling is needed.

The distribution of precipitation in space-time has long been known to display scaling, where the statistical properties of the distribution do not vary over some (large) range of scales. For example, a simple scaling law can relate world-wide extreme precipitation to the time scale ranging from minutes to years (Galmarini et al., 2004). Data sets displaying scaling may be either monofractal or multifractal in their distribution, depending on whether or not their scaling behaviour can be characterised by a single fractal dimension (Lovejoy and Schertzer, 2006).

The scale invariance of precipitation can be modeled as being multifractal in both time and space (Lovejoy and Schertzer, 2006; Olsson, 1995). Molnar and Burlando (2008) found differences in the multiscaling of winter and summer precipitation in Switzerland, with the summer precipitation showing strong multifractality and the winter precipitation being close to being monofractal. By statistically reproducing the observed multifractality, precipitation has been statistically downscaled to shorter time scales, while conserving observed scaling behaviours (Gaume et al., 2007; Seuront et al., 1999).

A disadvantage of statistical downscaling methods is that they require the existence of stationarity in the relationships between predictor and predictand variables (Fowler et al., 2007). In the case of multifractal downscaling, the requirement is for stationarity in the multifractality over time. Therefore, the objectives of this research are to determine:

– the existence of multiscaling in the temporal distributions of prairie snowfall,

– the existence of temporal trends in the multiscaling which will affect downscaling of prairie snowfall, and

– the effect(s) of any temporal trends in snowfall multiscaling on prairie hydrology caused by changes in the temporal frequency distribution of prairie snow accumulation.

K. R. Shook and
J. W. Pomeroy

2 Selection of data

Measurements of snowfall are highly influenced by wind induced undercatch (Goodison, 1978). Of equal importance for these analyses, the introduction of Nipher wind shields in Canadian use during the winter of 1960–1961 is known to have introduced
5 a discontinuity in snowfall data (Yang et al., 1999). To remove the influence of wind speed and shielding on the snowfall data, rehabilitated snowfall data were obtained from the Historical Adjusted Climate Database for Canada. These values have been adjusted for the effects of wind as described by Mekis and Hogg (1999).

Daily snowfall data for Calgary, Medicine Hat, Saskatoon, Regina, Indian Head and
10 Brandon were selected because they were widely dispersed throughout the prairies, had data preceding the 20th century, and the data collection sites were not moved during the period of record. The analyzed records span the years 1895–2003, with the exception of the Regina data which begin in 1898. The locations of the six sites on the Canadian prairies are shown in Fig. 1.

15 All analyses were performed using the open source statistical program R, which is described by Ihaka and Gentleman (1996). The program may be downloaded at http://www.r-project.org.

3 Scaling analyses

The presence of scaling in a time series is shown by the power spectrum of the data,
20 which will scale according to the relationship (Davis et al., 1994)

$$E(k) \propto k^{-\beta},$$ (1)

where:
$E(k)$ = power spectrum,
k = wave number,
25 β = constant.

The value of β indicates the behaviour of the underlying time series. If $\beta=0$, then the time series is entirely random. If $\beta < 1$, then the time series is stationary. If $\beta > 1$ then the time series is non-stationary (Davis et al., 1994).

For periods shorter than one month, i.e. for wavelengths greater than 1/31=0.032,
5 scaling behaviour ($\beta > 0$) was observed for all of the data sets. As shown in Fig. 2, the power spectrum for the Brandon daily snowfall displays scaling for time scales shorter than one month; at longer time scales, the scaling behaviour disappears. All of the snowfall datasets had values of $\beta < 1$ (mean=0.24, s.d.=0.06), indicating that the data are stationary. Although the frequency distribution of the snowfall may be stationary, it
10 does not necessarily follow that the temporal distribution of snowfall is also stationary.

Figure 3 shows that the magnitude of β for a given snowfall data set tends to be unstable over timescales on the order of decades, undergoing frequent statistically-significant shifts which indicate temporal variability in the scaling behaviour.

4 Multiscaling analysis

15 The existence of multiscaling in a data set can be determined in several ways; one of the simplest is through the moment scaling function $K(q)$ which is related to the normalised values of the data set, $\varepsilon(t)$, by (Olsson, 1995)

$$\langle \varepsilon_\lambda^q \rangle \approx \lambda^{K(q)} \tag{2}$$

where:
20 q = moment, and
λ = scale factor (ratio of scale of interest to size of entire data set).

The symbol $\langle \rangle$ refers to ensemble averaging the results of the calculations over all possible values of $\varepsilon(t)$. If the data are monofractal, then plots of $K(q)$ vs. q will describe a straight line. If the data are multifractal, then plots of $K(q)$ vs. q will exhibit curvature,
25 which can be quantified by the universal multifractal parameters (constants) α and C1

as described by (Seuront et al., 1999)

$$K(q) = \frac{C1}{\alpha - 1}(q^{\alpha} - q), \text{ for } \alpha \neq 1, q \geq 0. \tag{3}$$

The parameter α is an index of the intermittency of the data. The smaller the magnitude of α, the greater the intermittency of the data set (Finn et al., 2001). The parameter C1 is an index of the data's inhomogeneity, with greater C1 values representing greater inhomogeneity (Finn et al., 2001).

5   Scaling of extremes

The snowfall data sets show extreme positive skewness, because most of the daily snowfall data values are zero. The extreme values of multifractal data sets have very "fat" tails, compared to Gaussian distributions, the largest values fitting the scaling relationship defined by Olsson (1995) as

$$Pr(X > x) \propto x^{-q_D}, \tag{4}$$

where:
   X = a given value,
   x = a threshold value, and
   q_D = scaling exponent.
   The scaling exponent q_D has been identified as being the limiting moment beyond which moments will diverge from scaling relationships (Olsson, 1995). In practice, application of Eq. (4) is made more difficult by the fact that logarithmic plots of $Pr(X > x)$ vs. snowfall typically describe a curve, rather than having the abrupt "sill" described by Olsson (1995), which requires the use of a threshold or restricted range for computing q_D.
   Using the 100 largest values from each data set, the mean value of q_D for the snowfall datasets is 3.57 (s.d.=0.42). To ensure that Eq. (3) can be applied, the maximum

value of q used for all calculations of $K(q)$ in this research was set to 3.0. The values of $K(q)$ determined from the snowfall datasets typically agree very well with the values derived from the universal multiscaling relationship for values of q between 1 and 3.

Values of C1 and α for each data set were determined using the Double Trace Mo-
ment (DTM) method, as described by Olsson (1995) using $\lambda = n$ to $n/32$, where n = total number of points, based on the observed scaling over 1 to 31 days (32 being the closest power of 2), and $q=1$ to 3. The magnitudes of α for the snowfall datasets (mean=0.62, s.d.=0.07) and C1 (mean=0.46, s.d.=0.03) were similar to those found by Olsson (1995) of 0.626 and 0.44, respectively, for precipitation over time scales of
8 min to 11 days.

6 Multifractal stability

To test the temporal stability of the universal multifractal parameters, α and C1 were calculated for successive tenths of each snowfall data set. As shown in Fig. 4, the plots of $K(q)$ vs. q, and consequently values of α and C1, show frequent and significant changes throughout each of the datasets. Interestingly, the plots of $K(q)$ vs. q are only slightly curved, indicating that the snowfalls on the Canadian prairies, like Molnar and Burlando's observed Swiss snowfalls, are weakly multifractal.

Maximum and minimum values for α and C1 for each data set are listed in Table 1, together with the results of Mann-Kendall analyses of the parameters for trends at the 5% level. Many of the datasets show the presence of significant trends in their α values. Although none of the C1 parameters showed significant trends, and their mag-
nitudes showed less variability than did the values of α, the values of the parameters are inversely related, as shown in Fig. 5.

The hydrography of the Canadian prairies is very unusual because much of the land drains internally to small wetlands, rather than contributing to the flow of major rivers (Godwin and Martin, 1975). As described above, the hydrology of the region is also un-
usual as almost all surface runoff events are due to the spring melt of winter snowpacks,

rather than to runoff from rainfall. Therefore, it is difficult to link the multifractality of rainfall to that of streamflow records in this region, as was done in France by Tessier et al. (1996).

As snowpacks accumulate over an entire season, they would seem to be insensitive to the distribution of individual snowfall events. However, blowing snow events transport snow horizontally among landscape units and sublimation of blowing snow removes snow from the landscape. The moisture fluxes are highly dependent on wind speed, sublimation varying as the 5th power, and horizontal transport varying as the 4th power (Pomeroy and Gray, 1995; Essery, 2001). The fluxes also depend on the state of the snowpack, old snow being more resistant to erosion than new snow (Li and Pomeroy, 1997). The difference between the probability density function (PDF) of cumulative snowfall and that of the snow on the ground can be quite dramatic, as shown in Fig. 6. The site in Fig. 6a is near Banff, Alberta in a sheltered mountain valley and in this case wind redistribution is muted, but a shift is still evident possibly due to land use effects, though the PDF shape is conserved. The site in Fig. 6b is southeast of Edmonton, Alberta in the prairies where wind redistribution of snow can be significant and shows ablation of snowfall as well as a change in the shape of the PDF. Such a change is consistent with removal and redistribution of snow by wind. Therefore, it is anticipated that the temporal and frequency distributions of snowfall events will significantly affect the accumulation of snow which in turn will affect the distribution of runoff events.

The influence of snowfall disaggregation on snowcover generation was tested using the Cold Regions Hydrological Model (CRHM), a physically-based hydrological model developed at the Centre for Hydrology, University of Saskatchewan (Pomeroy et al., 2007). CRHM is able to accurately simulate the accumulation and sublimation of blowing snow of prairie landscapes and, being physically-based and requiring no calibration, is well-suited to simulation of changed conditions (Fang and Pomeroy, 2008).

Simulated snowfall data were created using the random multiplicative cascade method (Gaume et al., 2007), where the monthly snowfall is repeatedly subdivided over several generations. In the first generation, the snowfall is divided into two portions,

according to

$$S_{1,1} = S_0\eta, \; S_{1,2} = S_0(1 - \eta), \tag{5}$$

where:

S_0 = monthly snowfall,

$S_{1,1}$ = snowfall assigned to first piece in the first generation,

$S_{1,2}$ = snowfall assigned to second piece in the first generation, and

η = random number in the range 0–1.

The process is then repeated iteratively, doubling the number of pieces with each iteration. To produce daily values, 5 generations are used, creating 32 pieces, which were reduced to the required daily values for each month by

$$S_{\text{daily}} = S_{5,1..n} \left(\frac{S_0}{\sum_1^n S_{5,n}} \right), \tag{6}$$

where:

S_{daily} = daily snowfall values for a given month,

S_5 = the 5th generation, and

n = number of days in given month.

By manipulating the distribution of η, data series having varying values of α and C1 can be generated. As shown in Fig. 7, increasing the magnitude of α while decreasing the magnitude of C1 results in snowfall distributions which tend to produce more frequent, smaller events which are distributed more evenly in time. In both cases the total snowfall is 19.5 mm. Snowfall events having large values of α will result in snowpacks whose surfaces are relatively new and therefore more subject to blowing, at any given time.

Full Screen / Esc

Printer-friendly Version

Interactive Discussion

7 Simulation

The basin simulated by the model is of a typical small prairie stream, consisting of upland fallow and stubble fields which drain runoff into a grassed intermittent stream channel. It is modeled on Creighton Tributary at Bad Lake, Saskatchewan. The ability of CRHM to produce accurate simulations of snow accumulations at this location was demonstrated by Pomeroy et al. (2007). Because of the shortness of the recorded data set (less than 20 years), meteorological data from Saskatoon were used in this study. Although Saskatoon is approximately 150 km northeast of Creighton Tributary the intention is to simulate the effects of downscaling, rather than to accurately model the hydrology of a particular location.

CRHM uses Hydrological Response Units (HRU) to simulate the behaviour of each of the basins's sub-regions. Within each HRU all state variables, forcings, and parameters are assumed to be spatially uniform. An important feature of CRHM is that HRUs may be linked in a variety of ways. Although runoff drains to the stream channel, the action of blowing will transport snow from the fallow field to the stubble field, and from both the stubble and fallow fields to the grassed channel, based on their relative surface roughnesses. Traditional hydrological models, where connectivity is based on surface water drainage, cannot properly capture the redistribution of wind-blown snow.

Although CRHM uses daily snowfall values, the model is run on an hourly time step and requires hourly values of air temperature, relative humidity, wind speed, rainfall, and incoming solar radiation. Each simulation was run for the period 1960–2006, for which good values of the hourly forcing variables other than solar radiation were available. Daily incoming shortwave solar radiation was estimated from air temperature using the method ofAnnandale et al. (2001), and downscaled to hourly values as described in Shook and Pomeroy (2010). Because the snowfall downscaling process is stochastic, the set of downscaled data will depend on the particular set of random values of η generated from the specified distribution. To reduce the effects of the finite length of the simulations, fifteen realizations were run for each disaggregation,

Full Screen / Esc

consisting of a single set of lognormal parameters specifying the frequency distribution of η. The downscaled datasets had fairly consistent values of α and C1 over the realizations, their mean coefficients of variation being 0.07 and 0.03, respectively. As shown in Fig. 8, the ranges of α and C1 values, and their relationship to each other,
5 are similar for the synthetic data and for the observed Saskatoon daily snowfall values.

8 Results

The CRHM runs produced snow accumulations for each HRU for which mean daily snow water equivalent (SWE) values were computed over each set of realizations. As shown in Fig. 9, the variation in α and C1 caused variation in the timing and magnitudes
10 of snow accumulation and melt for each HRU. The accumulation on the stubble HRU was least affected, probably because it both receives and transmits blowing snow.
    The effect of variation in the multifractal parameters on the mean peak accumulation of SWE is shown in Fig. 10. The plots show that increased values of α in the snowfall time series result in linearly increased values of mean peak SWE on the grass HRU,
15 decreased values on the fallow field and largely unchanged values on the stubble HRU. These results are consistent with the assumption of increased blowing snow events resulting from increased values of α, as noted above.

9 Summary and conclusions

Analyses of daily snowfall on the Canadian prairies determined that the datasets ex-
20 hibit multifractality at temporal scales shorter than one month, and that the multiscaling shows evidence of trends for decreasing intermittency of snowfall over the last century at the majority of sites tested. The transformation of snowfall into snow on the ground via redistribution and ablation processes means that frequency distributions of snowfall cannot be used directly to create distributions of snow on the ground. Blowing snow

K. R. Shook and
J. W. Pomeroy

Full Screen / Esc

and snow ablation simulations driven by stochastic or measured snowfall estimates can estimate snow on the ground using physically-based calculations. Such simulations demonstrate that the timing and quantity of the spring snowmelt is affected by the observed multiscaling of daily snowfalls, probably because the effects of blowing snow on snowfall accumulation are strongly influenced by the timing of snowfall. Because the majority of annual runoff in this region is typically the result of spring snowmelt, and because climate models require downscaling to produce daily snowfalls, the variability in the multiscaling of prairie snowfalls represents an additional source of uncertainty in determining the hydrological effects of climate model outputs. This can be compensated for in historical analyses but at the present time there is no method to identify likely scaling trends for future scenarios.

References

Annandale, J. G., Jovanovic, N. Z., Benadé, N., and Allen, R. G.: Software for missing data analysis of Penman-Monteith reference evapotranspiration, Irrigation Sci., 21, doi:10.1007/s0027110100047, 57–67, 2001. 1288

Davis, A., Marshak, A., Wiscombe, W., and Calahan, R.: Multifractal characterizations of nonstationarity in geophysical fields: Observed, retrieved or simulated, J. Geophys. Res., 49(D4), 8055–8072, 1994. 1282, 1283

Essery, R.: Spatial statistics of windflow and blowing-snow fluxes over complex topography, Bound-Lay. Meteor., 100, 131–147, 2001. 1286

Fang, X. and Pomeroy, J.: Drought impacts on Canadian prairie wetland snow hydrology, Hydrol. Processes, 22(15), 2858–2873, doi:10.1002/hyp.7074., 2008. 1280, 1286

Finn, D., Lamb, B., Leclerc, M. Y., Lovejoy, S., Pecknold, S., and Schertzer, D.: Multifractal

Analysis of Line-Source Plume Concentration Fluctuations in Surface-Layer Flows, J. Appl. Meteor., 40, 229–245, 2001. 1284

Fowler, H. J., Blenkinsop, S., and Tebaldi, C.:. Review Linking climate change modelling to impacts studies: recent advances in downscaling techniques for hydrological modelling, Int. J. Climatol., 1578, 1547–1578, doi:10.1002/joc, 2007. 1281

Galmarini, S., Steyn, D. G., and Ainslie, B.: The scaling law relating world point-precipitation records to duration, Int. J. Climatol, 24(5), 533–546, 2005.

Gaume, E., Mouhous, N., and Andrieu, H.: Rainfall stochastic disaggregation models: Calibration and validation of a multiplicative cascade model, Adv. Water Resour., 30, 1301–1319, 2007. 1281, 1286

Godwin, R. B. and Martin, F. R. J.: Calculation of gross and effective drainage areas for the Prairie Provinces. In: Canadian Hydrology Symposium – 1975 Proceedings, 11–14 August 1975, Winnipeg, Manitoba. Associate Committee on Hydrology, National Research Council of Canada, pp. 219–223, 1975. 1285

Goodison, B.: Accuracy of Canadian Snow Gage Measurements, J. Appl. Meteorol., 17, 1542–1548, 1978. 1282

Hanssen-Bauer, I., Førland, E., Haugen, J., and Tveito, O.: Temperature and precipitation scenarios for Norway: comparison of results from dynamical and empirical downscaling, Climate Res., 25(2001), 15–27, doi:10.3354/cr025015, 2003.

Ihaka, R. and Gentleman, R.: R: A language for data analysis and graphics, J. Comput. Graphical Statist., 5(3), 299–314, 1996. 1282

Li, L. and Pomeroy, J. W.: Estimates of Threshold Wind Speeds for Snow Transport Using Meteorological Data, J. Appl. Meteorol., 36(3), 205–213, doi:10.1175/1520-0450(1997)036<0205:EOTWSF>2.0.CO;2, 1997. 1286

Lovejoy, S. and Schertzer, D.: Multifractals, cloud radiances and rain, J. Hydrol., 322(1–4), 59–88, doi:10.1016/j.jhydrol.2005.02.042, 2006. 1281

Mekis. E. and Hogg, W. D.: Rehabilitation and Analysis of Canadian Daily Precipitation Time Series, Atmos. Ocean, 44(2), 53–85, 1999. 1282

Molnar, P. and Burlando, P.: Variability in the scale properties of high-resolution precipitation data in the Alpine climate of Switzerland, Water Resour. Res., 44, W10404, doi:10.1029/2007WR006142, 2008. 1281, 1285

Olsson, J.: Limits and characteristics of the multifractal behaviour of a high-resolution rainfall time series, Nonlin. Processes Geophys., 2, 23–29, 1995,

Temporal variability of snowfall multiscaling

K. R. Shook and
J. W. Pomeroy

http://www.nonlin-processes-geophys.net/2/23/1995/. 1281, 1283, 1284, 1285

Pomeroy, J. W. and Gray, D. M.: Snowcover accumulation, relocation and management, National Hydrology Research Institute Science Report No. 7. NHRI, Environment Canada, Saskatoon, 144 pp., 1995. 1280, 1286

5 Pomeroy, J. W., Gray, D. M., and Landine, P. G.: The Prairie Blowing Snow Model: characteristics, validation, operation, J. Hydrol., 144, 165–192, 1993. 1280

Pomeroy, J. W., Gray, D. M., Brown, T., Hedstrom, N. R., Quinton, W. L., Granger, R. J., and Carey, S. K.: The cold regions hydrological model: a platform for basing process representation and model structure on physical evidence, Hydrol. Processes, 21, 2650–2667, 2007.

10 1286, 1288

Shook, K. and Gray, D. M.: Synthesizing Shallow Seasonal Snow Covers, Water Resour. Res., 33(3), 419–426, 1997. 1280

Shook, K. and Pomeroy, J. W.: Synthesis of Incoming Shortwave Radiation for Hydrological Simulation, Hydrol. Res., in review, 2010. 1288

15 Seuront, L., Schmitt, F., Langadeuc, Y., Schertzer, D., and Lovejoy, S.: Universal multifractal analysis as a tool to characterize multiscale intermittent patterns: example of phytoplankton distribution in turbulent coastal waters, J. Plankton Res., 21(5), 877–922, 1999. 1281, 1284

Tessier, Y., Lovejoy, S., Hubert, P., Schertzer, D., and Pecknold, S.: Multifractal analysis and modeling of rainfall and river flows and scaling, causal transfer functions, J. Geophys. Res.,

20 101(D21), 26427–26440, 1996. 1286

Wilby, R. and Wigley, T.: Downscaling general circulation model output: a review of methods and limitations, Prog. Phys. Geog., 21(4), 530–548, doi:10.1177/030913339702100403, 1997. 1280

Yang, D, Goodison, B. E., Metcalfe, J. R., Louie, P., Leavesley, G., Emerson, D., Hanson,

25 C. L., Golubev, V. S., Elomaa, E., Gunther, T., Pangburn, T., Kang, E., and Milkovic, J.: Quantification of precipitation measurement discontinuity induced by wind shields on national gauges, Water Resour. Res., 35(2), 491–508, 1999. 1282

Temporal variability of snowfall multiscaling

K. R. Shook and
J. W. Pomeroy

Title Page

Abstract | Introduction

Conclusions | References

Tables | Figures

◄◄ | ►►

◄ | ►

Back | Close

Full Screen / Esc

Printer-friendly Version

Interactive Discussion

Table 1. Temporal variability in values of α and C1, and the results of Mann-Kendall trend analyses.

Site	α			C1		
	Min	Max	Mann-Kendall	Min	Max	Mann-Kendall
Calgary	0.30	0.55	Positive trend	0.48	0.57	No trend
Medicine Hat	0.29	0.54	Positive trend	0.51	0.55	No trend
Indian Head	0.20	0.58	Positive trend	0.46	0.57	No trend
Regina	0.34	0.65	No trend	0.43	0.51	No trend
Saskatoon	0.33	0.63	Positive trend	0.42	0.54	No trend
Brandon	0.25	0.48	No trend	0.52	0.60	No trend
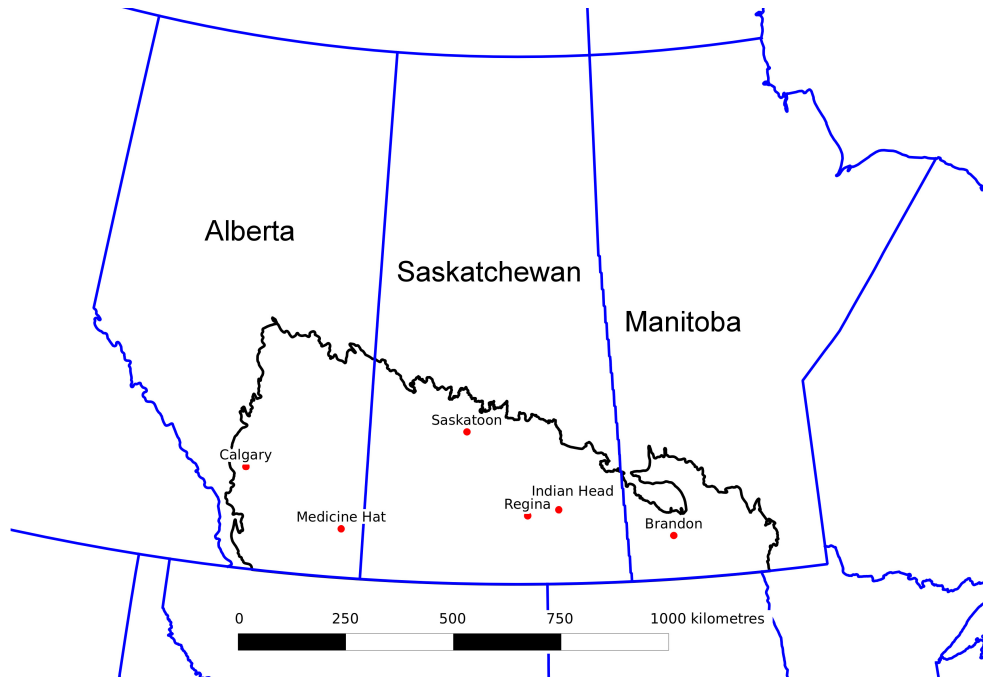
Fig. 1. Location of the study sites in Western Canada. The prairie ecoregion in Canada is outlined.
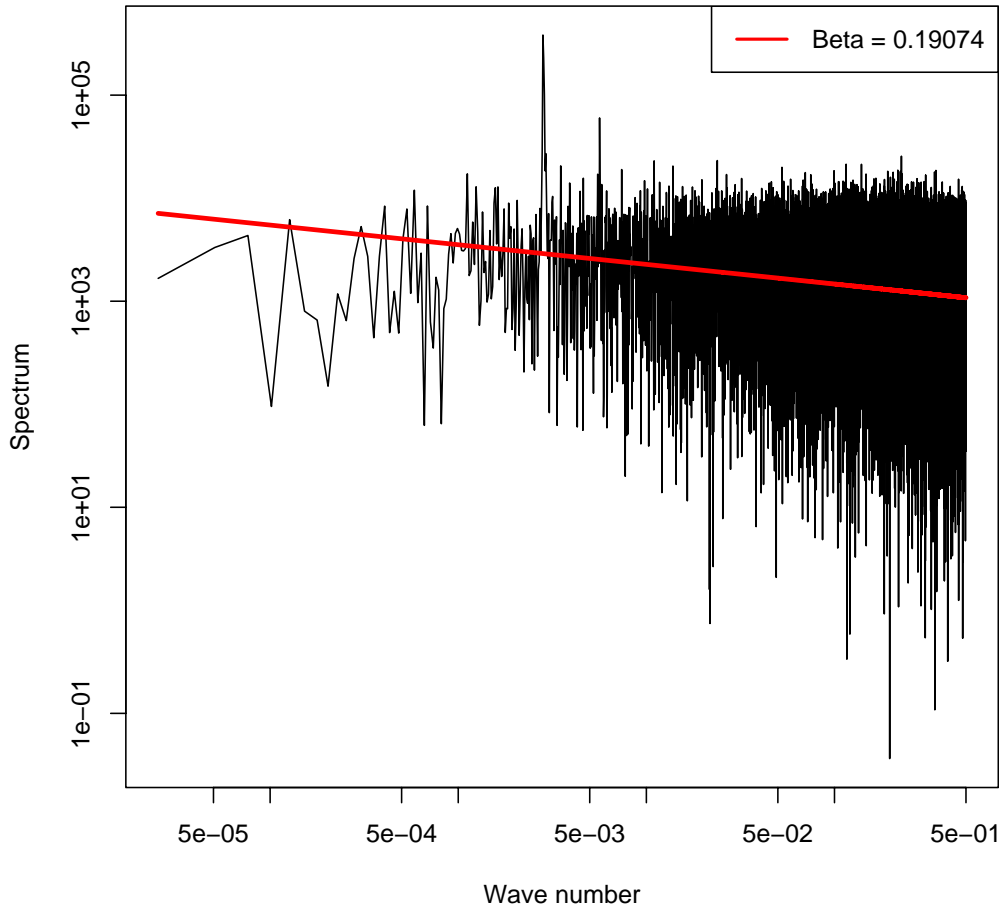
Fig. 2. Power spectrum of Brandon daily snowfalls. The best-fit line corresponds to Eq. (1), for wavelengths greater than 0.032.
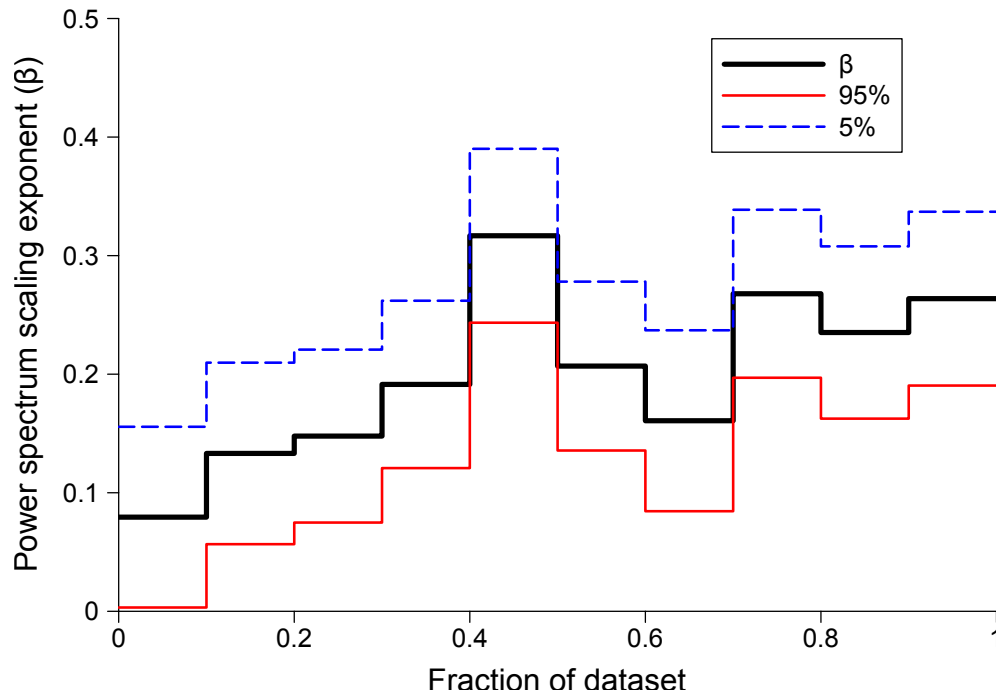
Fig. 3. Temporal variability of power spectrum scaling exponent for Brandon daily snowfall over the period 1895 to 2003. The 5% and 95% confidence levels of the regressions are also plotted.
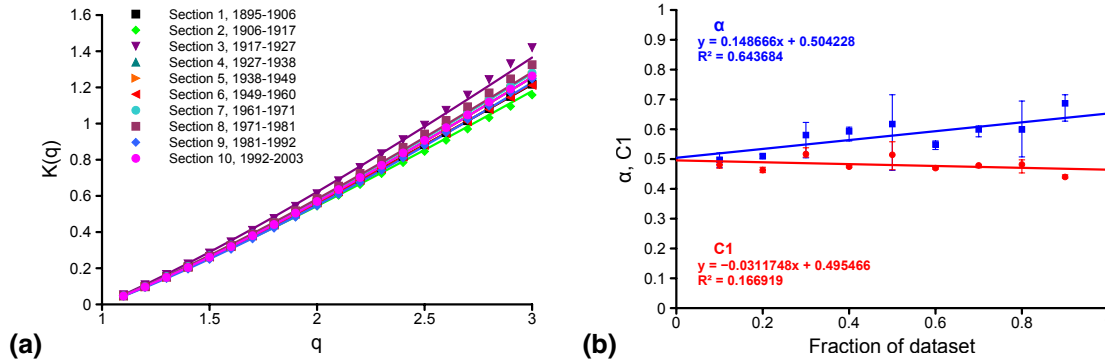
Fig. 4. Temporal variability of mulitfractality of Medicine Hat daily snowfall data, 1895–2003. **(a)** $K(q)$ vs. q for all sections (tenths) of the data series. Points are empirical values, lines are universal multiscaling relationships. **(b)** Variation in values of α and C1 by fraction of the data series. The vertical bars represent the maximum and minimum α and C1 values computed over each interval.
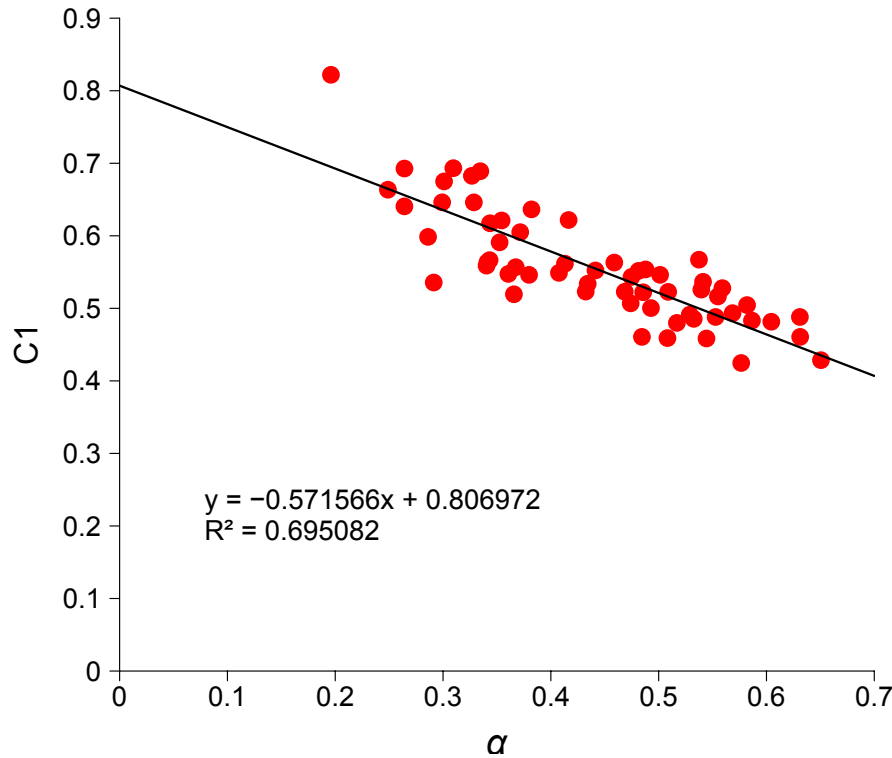
Fig. 5. Relationship between C1 and α for all snowfall datasets divided into tenths.

$y = -0.571566x + 0.806972$
$R^2 = 0.695082$
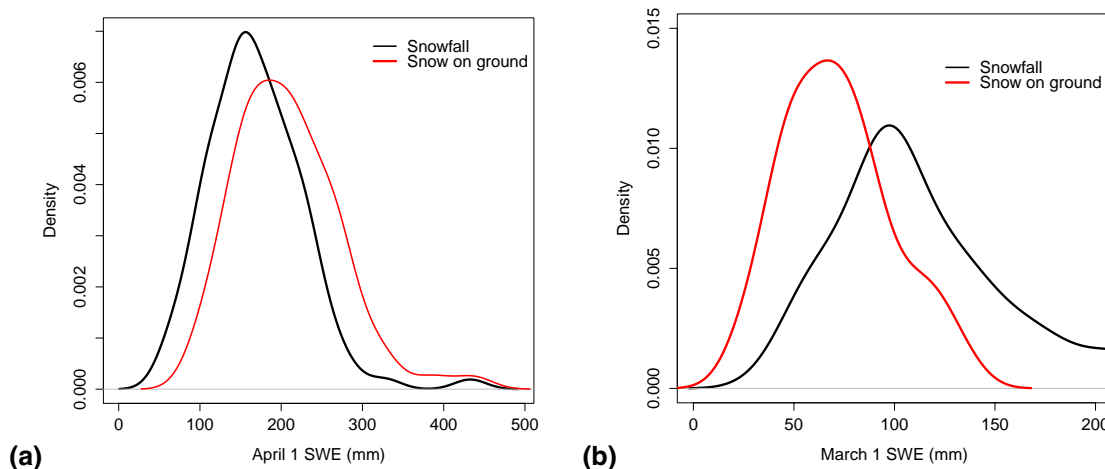
Fig. 6. (a) Density plot of 1 April cumulative seasonal snowfall at Banff, AB and snow on ground at Bow River snow course (1937–2009). The horizontal distance between the two sites is approximately 3 km, and the difference in elevation is less than 200 m. **(b)** Density plot of 1 March cumulative seasonal snowfall at Edmonton, AB and snow on ground at Bellis snow course (1974–2009). The horizontal distance between the two sites is approximately 15 km, and the difference in elevation is less than 60 m.
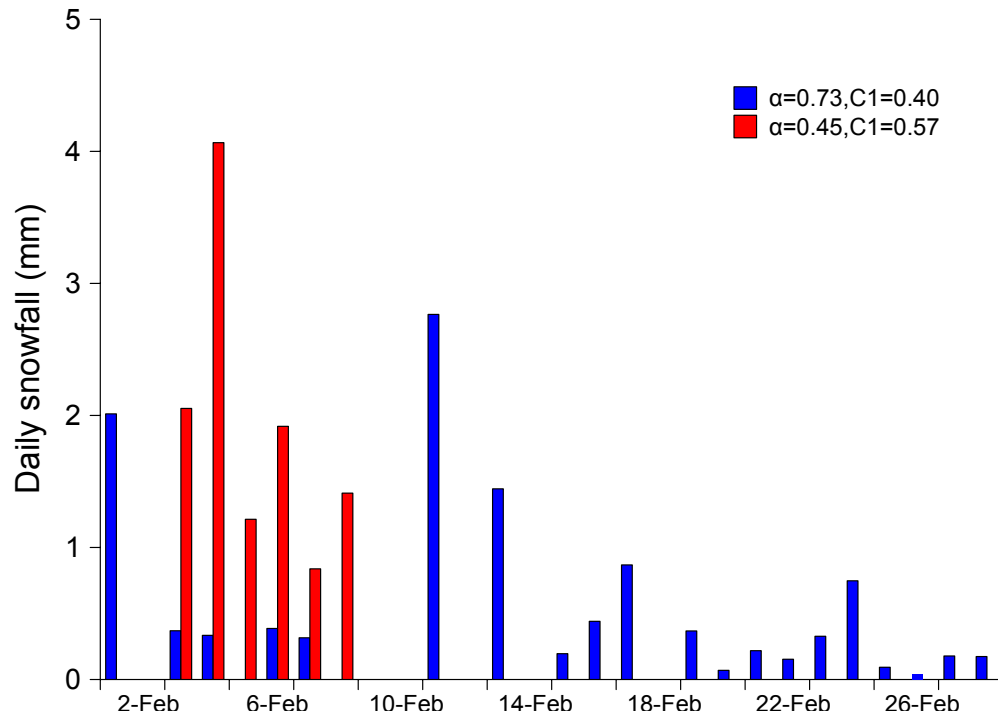
Fig. 7. Realizations of daily distributions of monthly snowfall for Saskatoon, February 2006.
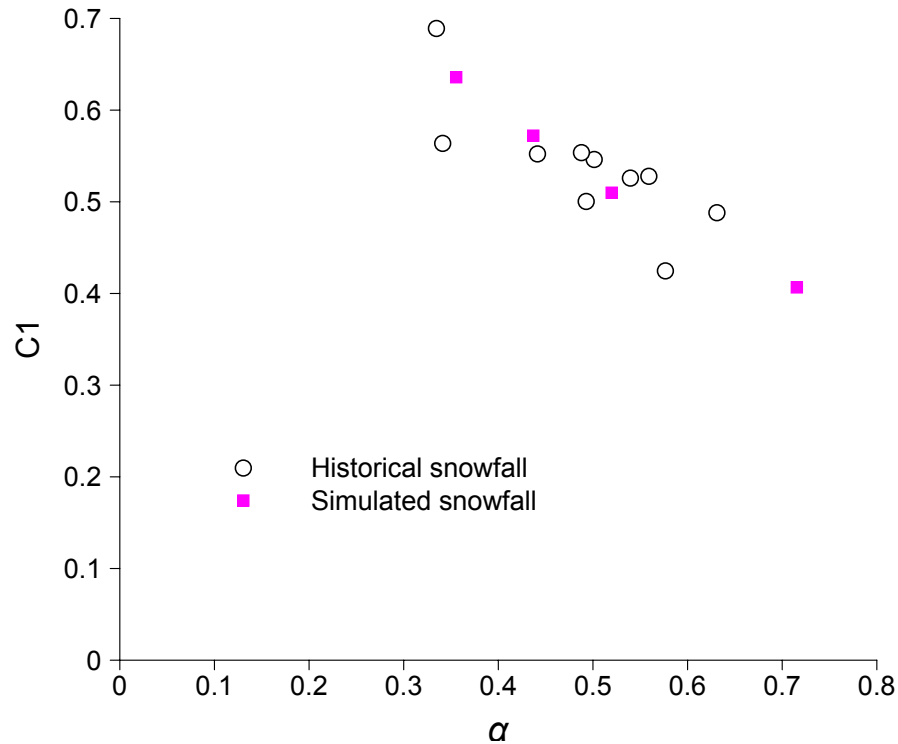
Fig. 8. Mean values of α and C1 derived from Saskatoon daily snowfall (divided into tenths) and from simulated daily snowfall data downscaled from measured monthly snowfalls.

Title Page

Abstract   Introduction

Conclusions   References

Tables   Figures

◄◄   ►►

◄   ►

Back   Close

Full Screen / Esc

Printer-friendly Version

Interactive Discussion

(a) Fallow HRU. **(b)** Stubble HRU. **(c)** Grass HRU.
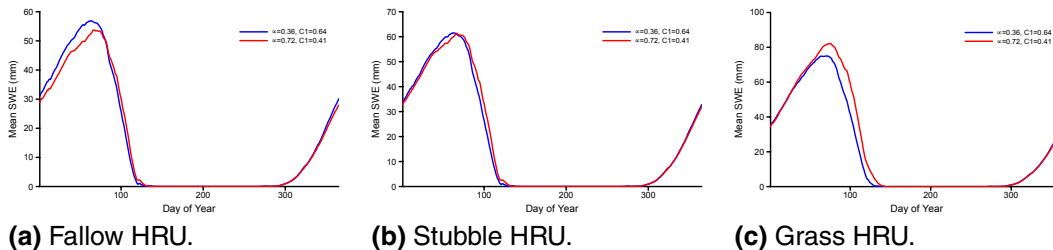
Fig. 9. Mean CRHM simulated snowcover accumulations for three HRUs, based on measured monthly snowfall downscaled to daily values. The curves represent accumulations from down-scaled data having α and C1 values of 0.36 and 0.64, and 0.72 and 0.41, respectively, which correspond to the extremes of the values measured in sub-sets of historical data.
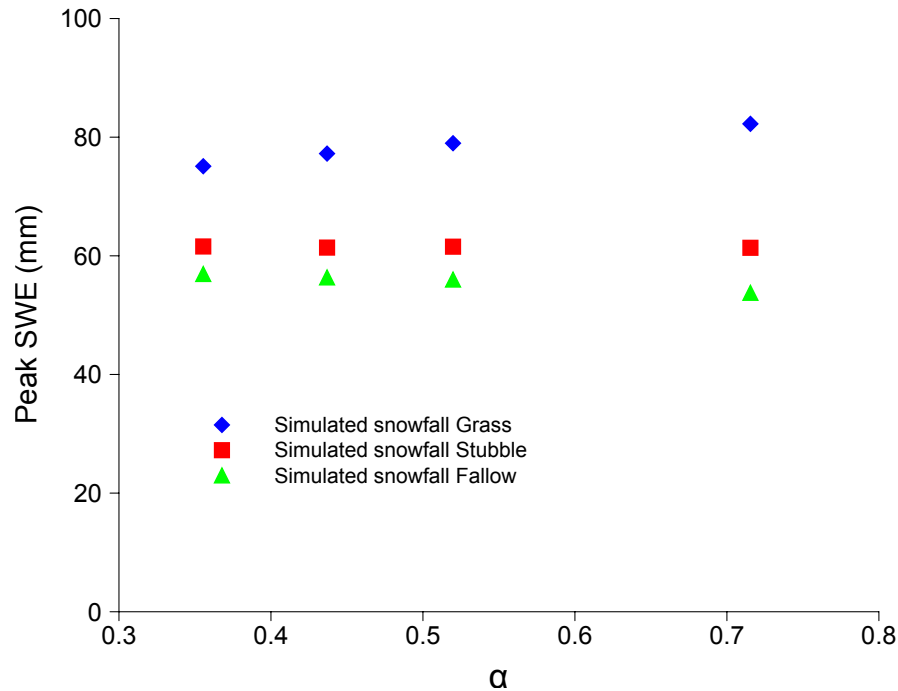
Fig. 10. Variation in simulated peak snowfall vs. α for simulated and measured snowfalls on fallow, stubble and grass HRUs. Measured snowfall data from Saskatoon, SK, 1960–2006.